Thermo-hydro-mechanical (THM) modeling of borehole breakouts for in-situ stress determination in geothermal exploration

Hua, Zhang
Department of Petroleum Engineering, University of Wyoming, Laramie, WY, USA
Shunde, Yin
Department of Civil and Environmental Engineering, University of Waterloo, Waterloo, Canada
Maurice B. Dusseault
Department of Earth and Environmental Science, University of Waterloo, Waterloo, Canada

Summary

The determination of in-situ stresses is important in Enhanced Geothermal System (EGS) energy development. Large-scale stress changes take place during EGS, affecting rock mass permeability, expecially in naturally fractured rock masses, and potentially even triggering felt microseismic activity. Good predictive modeling is vital for decisions on project viability and environmental impact, therefore good stress data are vital. Hydraulic Fracturing (HF) is a widely accepted technique for in-situ stress determination, but is time-consuming and expensive because of rig time involved in lowering the tools to take measurements. In contrast, taking advantage of the shape of borehole breakouts measured from widely-available caliper and image logs to estimate in-situ stress in deep hot rocks is more economical, requires no extra rig time, and is thus an attractive alternative. Four-arm caliper data and image logs are standard borehole geophysical logs, and more sophisticated logs may be used if more data are required (such as in a research borehole or the first several boreholes in a multi-well EGS program).

By finite element modeling of borehole breakouts considering thermoporoelasticity, the authors simulate the process of borehole breakouts in terms of initiation, development, and stabilization under Mogi-Coulomb criterion and end up with the shape of borehole breakouts. Artificial neural network provides such a tool to establish the relationship between in situ stress and shape of borehole breakouts, which can be used to determine in situ stress based on different shape of borehole breakouts by inverse analysis. In this paper, two steps are taken to determine in situ stress by inverse analysis. First, sets of finite element modeling provide sets of data on in situ stress and borehole breakout measures considering the influence of drilling fluid temperature and pore pressure, which will be used to train an artificial neural network that can eventually represent the relationship between the in situ stress and borehole breakout measures. Second, for a given measure of borehole breakouts in a certain drilling fluid temperature, the trained artificial neural network will be used to predict the corresponding in situ stress. Results of numerical experiments show that the inverse analysis based on finite element modeling of borehole breakouts and artificial neural network is a promising method to determine in situ stress.

Theory / Method / Workflow

Rock Failure Criterion

The Mogi–Coulomb criterion is used to analyze wellbore stability with the effect of intermediate principal stress on rock strength considered.

$$\tau'_{oct} = a + \sigma'_{m,2} \qquad (1)$$

in which

$$\tau'_{oct} = \frac{1}{3}\sqrt{(\sigma'_1 - \sigma'_2)^2 + (\sigma'_2 - \sigma'_3)^2 + (\sigma'_3 - \sigma'_1)^2}$$

$$\sigma'_{m,2} = \frac{\sigma'_1 + \sigma'_3}{2}$$

$$a = \frac{2\sqrt{2}}{3} c\cos\varphi$$

$$b = \frac{2\sqrt{2}}{3} \sin\varphi$$

where $\sigma'_1, \sigma'_2, \sigma'_3$ are effective principal stresses, c is the cohesive strength, φ is the internal friction angle.

Simulation of Thermoporoelastic Borehole Breakouts by the Finite Element Method

Borehole breakouts occur as a series of successive spalls in the direction of the local minimum principal stress that result from shear failure subparallel to the free surface of the borehole wall.

Fig.1 shows the schematic of a typical borehole breakout process, where (1), (2), (n)represent the failure regions of each cyclic process, respectively; 1, 2, n represent the surface of a breakout of each cyclic process, respectively.

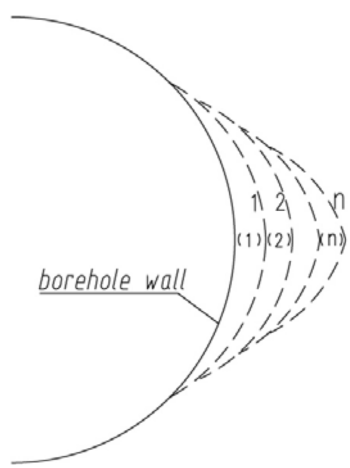

Fig.1. Schematic of a borehole breakout process

Finite Element Implementation

For the compressible fluid flowing through the saturated non-isothermal deformable porous medium, in the form of displacements, pressure and temperature as unknowns, the governing equations can be described as follows.

$$G\nabla^2\boldsymbol{u} + (G + \lambda)\nabla div\boldsymbol{u} - \left(1 - \frac{K}{K_m}\right)\nabla\boldsymbol{p} - K\beta_s\nabla\boldsymbol{T} + \boldsymbol{f}^u = 0 \qquad (2)$$

$$\left(1-\frac{K}{K_m}\right) div\boldsymbol{u_t} + \left[\frac{1-\phi}{K_m}+\frac{\phi}{K_f}+\frac{1}{(3K_m)^2}i^T D i\right]\boldsymbol{p_t} + \frac{k}{\mu}\nabla^2\boldsymbol{p} - \left[\phi\beta_f + (1-\phi)\beta_s + \frac{\beta_s}{9K_m}i^T D i\right]\boldsymbol{T_t} + \boldsymbol{f}^p = 0 \tag{3}$$

$$T\left[(1-\phi)\frac{\rho_s c_s}{K_m} + \phi\frac{\rho_f c_f}{K_f}\right]\boldsymbol{p_t} + \left[(1-\phi)\rho_s c_s + \phi\rho_f c_f - T(1-\phi)\rho_s c_s\beta_s - T\phi\rho_f c_f\beta_f\right]\boldsymbol{T_t} + \lambda_T\nabla^2\boldsymbol{T} + \boldsymbol{f}^T = 0 \tag{4}$$

The Galerkin finite element method is used to approximate these governing equations. The final form of the FEM solution to the thermoporoelastic equations is as follows:

$$\begin{bmatrix} M & -C_{sw} & -C_{sT} \\ 0 & H_{ww} & 0 \\ 0 & 0 & H_{TT} \end{bmatrix}\begin{Bmatrix} u \\ p \\ T \end{Bmatrix} + \begin{bmatrix} 0 & 0 & 0 \\ C_{sw}^T R_{ww} & -C_{wT} & \\ 0 & C_{Tw}R_{TT} & \end{bmatrix}\begin{Bmatrix} u_t \\ p_t \\ T_t \end{Bmatrix} = \begin{Bmatrix} f^u \\ f^p \\ f^T \end{Bmatrix} \tag{5}$$

To integrate the above equations with respect to time (θ method), the equation becomes:

$$\begin{bmatrix} M & -C_{sw} & -C_{sT} \\ C_{sw}^T R_{ww} + \Delta t\theta H_{ww} & & -C_{wT} \\ 0 & & C_{Tw}R_{TT} + \Delta t\theta H_{TT} \end{bmatrix}\begin{Bmatrix} \Delta u \\ \Delta p \\ \Delta T \end{Bmatrix} = \begin{Bmatrix} \Delta f^u \\ \Delta t\theta f_1^p + \Delta t(1-\theta)f_0^p - \Delta t H_{ww} p_0 \\ \Delta t\theta f_1^T + \Delta t(1-\theta)f_0^T - \Delta t H_{TT} T_0 \end{Bmatrix} \tag{6}$$

Inverse Analysis by Artificial Neural Network

An ANN includes an input layer, a hidden layer and an output layer. A schematic of a three-layer neural network model and a single artificial neuron is shown in Fig.2.

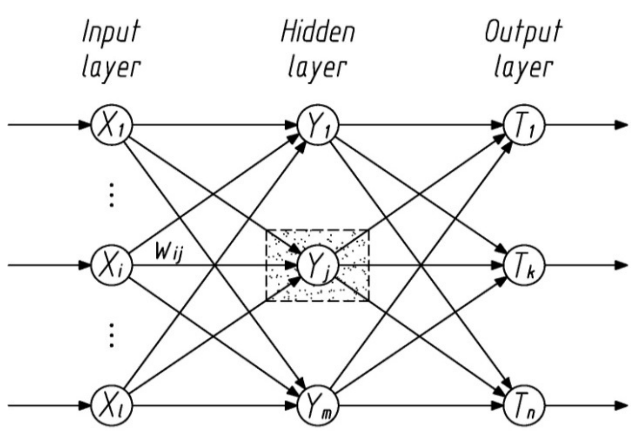

(A)

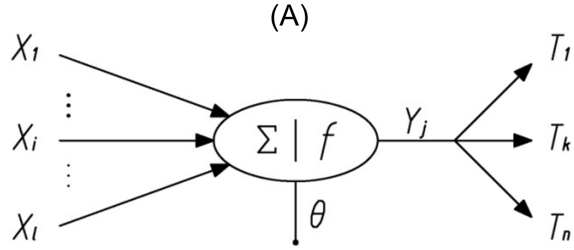

(B)

Fig.3. (A) Schematic diagram of ANN and (B) a single artificial neuron

For a single artificial neuron, Y_j can be expressed as

$$Y_j = f\left(\sum_{i=1}^{l} w_{ij} X_i + \theta\right) \quad (7)$$

Results, Observations, Conclusions

Numerical experiments of finite element modeling of borehole breakouts show the contrasting tendency of breakouts shape with different in-situ stress conditions. It was also found that the depth of breakouts increases until a stable state is reached, but the width of breakouts remains unchanged in the process of borehole breakouts. For different temperatures of the drilling fluid with respect to the rock mass, the higher the drilling fluid temperature, the more severe borehole breakouts will be.

Numerical experiments show that inverse analysis by ANN based on thermoporoelastic borehole breakout modeling is a promising method to determine in-situ stress. In the numerical experiments in this study, the finite element models produce the simulated breakouts. However, anisotropy and plastic behavior are not considered in this work, thus its application to more brittle rock such as those encountered in EGS situations is more likely to lead to useful stress estimates. Furthermore, additional constraints (e.g. good measurements of σ_h) will aid in the generation if better ANN results.

Novel/Additive Information

Taking advantage of the shape of borehole breakouts measured from widely-available caliper and image logs to estimate in-situ stress in deep hot rocks is more economical, requires no extra rig time, and is thus an attractive alternative. Four-arm caliper data and image logs are standard borehole geophysical logs, and more sophisticated logs may be used if more data are required (such as in a research borehole or the first several boreholes in a multi-well EGS program).

References

1. Al-Ajmi A.M., Zimmerman R.W. (2005). "Relation between the Mogi and the Coulomb failure criteria." Int J Rock Mech Min Sci, 42:431–9

2. Bell J.S., Gough D.I. (1979). "Northeast-Southwest compressive stress in Alberta: evidence from oil wells." Earth Planet Sci Lett, 45:475–82.

3. Carr W.J. (1974). "Summary of tectonic and structural evidence for stress orientation at the Nevada Test Site." Open file report, US Geological Survey, Denver, Colorado, p.74-176.

4. Chen Y., Deng L. (2014). "The best learning order inference based on blue-red trees of rule-space model for social network." International Journal of Computational Science and Engineering, Vol. 9, No. 3, pp.155-164.

5. Cox J.W. (1970). "The high resolution dip meter reveals dip-related borehole and formation characteristics." Trans 11th SPWLA logging symposium, D1-D26.

6. Haimson B.C., Herrick C.G. (1985). "In situ stress evaluation from borehole breakouts experimental studies." In: Proceedings of the 26th US rock mechanics symposium; 1985. Rotterdam: Balkema, 1207-1218.

7. Haimson B.C., Herrick C.G. (1986). "Borehole breakouts - a new tool for estimating in situ stress?" In: Proceedings of the first international symposium on rock stress and rock stress measurement. Lulea: Centek Publications, 271-281.
8. Haimson B.C., Chang C. (2000). "A new true triaxial cell for testing mechanical properties of rock, and its use to determine rock strength and deformability of Westerly granite." Int J Rock Mech Min Sci,37:285–96.
9. Haimson B.C., Chang C. (2002). "True triaxial strength of the KTB amphibolite under borehole wall conditions and its use to estimate the maximum horizontal in situ stress." J Geophys Res, 107:2257–2270.
10. Haimson B.C. (2007). "Micromechanisms of borehole instability leading to breakouts in rocks." Int J Rock Mech Min, 44:157–173.
11. Han H., Yin S., (2018). "Determination of Geomechanical Properties and In-situ Stress from Borehole Deformation." Energies. Vol. 11: 131.
12. Hickman S.H., Healy J.H., Zoback M.D. (1985). "In situ stress, natural fracture distribution and borehole elongation in Auburn geothermal well, Auburn, New York." J Geophys Res, 90:5497–5512.
13. Hickman S.H., Zoback M.D. (2004). "Stress orientations and magnitudes in the SAFOD pilot hole." Geophys Res Lett,31: L15S12.
14. Leeman E.R. (1964). "The treatment of stress in rock: I. The rock stress measurement: II. Borehole rock stress measuring instrument: III. The results of some rock stress investigations." J S Afr Inst Min Metall,65(45-114):254–84.
15. Mastin L. (1984). "The development of borehole breakouts in sandstone." M.S. thesis, Stanford Univ., Stanford, Calif.
16. McCulloch W.S., Pitts W.H. (1943). "A logical calculus of the ideas immanent in nervous activity." Bulletin of Mathematical Biology, Vol. 5, Nos. 1/2, pp.115-133.
17. Mogi K. (1971). "Fracture and flow of rocks under triaxial compression." J Geophys Res, 76: 1255–69.
18. Mostafa Gomar, Iraj Goodarznia, Seyed Reza Shadizadeh (2014). "Transient thermo-poroelastic finite element analysis of borehole breakouts." International Journal of Rock Mechanics & Mining Sciences, 71 (2014) 418–428.
19. Papamichos E. (2010). "Borehole failure analysis in a sandstone under anisotropic stresses." Int J Numer Anal Meth Geomech, 34:581– 603.
20. Shamir G., Zoback M.D. (1992). "Stress orientation profile to 3.5 km depth near the San Andreas Fault at Cajonpas, California." J Geophy Res, 97:5059–5080.
21. Yan G., Zhao H., Chen Y., Ren Y. (2013). "The self-adaptive integrated algorithm on time-sensitive cluster evolution tracking." International Journal of Embedded Systems, Vol. 5, No. 4, pp.248-263.
22. Yin S. (2008). "Geomechanics-Reservoir Modeling by Displacement Discontinuity-Finite Element Method." University of Waterloo. PhD: 22-23.
23. Yin S., Towler B.F., Dusseault M.B., Rothenburg L. (2010). "Fully coupled THMC modeling of wellbore stability with thermal and solute convection considered." Transport in Porous Media. Vol. 84, pp. 773-798.
24. Yuan S.C., Harrison J.P. (2006). "Modeling breakout and near-well fluid flow of a borehole in an anisotropic stress field." 41st ARMA/USRMS 06–1157.
25. Zhang H., Yin S., Aadnoy B.S. (2018). "Finite-element modeling of borehole breakouts for in situ stress determination." Int. J. Geomech., 18(12): 04018174.
26. Zhang H., Yin S., Aadnoy B.S. (2018). "Poroelastic modeling of borehole breakouts for in-situ stress determination by finite element method." J Petroleum Science and Engineering, 162 (2018), 674-684.
27. Zhang H., Yin S., Aadnoy B.S. (2019). "Numerical investigation of the impacts of borehole breakouts on breakdown pressure." Energies, 2019, 12, 888.
28. Zhang S., Yin S. (2014). "Determination of horizontal in-situ stresses and natural fracture properties from wellbore deformation." International Journal of Oil, Gas and Coal Technology, Vol. 7, No. 1, pp.1-28.
29. Zhang S., Yin S. (2015). "Determination of earth stresses using inverse analysis based on coupled numerical modeling and soft computing." International Journal of Computer Applications in Technology, Vol. 52, No. 1, pp.18-28.
30. Zheng Z., Kemeny J., Cook NGW (1989)."Analysis of borehole breakouts." J Geophys Res, 94:7171–82.
31. Zoback M.D., Moos D.L., Mastin L., Anderson R.N. (1985). "Wellbore breakout and in-situ stress." J Geophys Res, 90:5523–38.
32. Zoback M.D., Vernik L. (1992). "Estimation of maximum horizontal principal stress magnitude from stress-induced well bore breakouts in the Cajon Pass scientific research borehole." J Geophys Res, 97:5109–5119.